Received: 3 February 2021 | Revised: 25 May 2021 | Accepted: 9 July 2021

DOI: 10.1111/clr.13812

ORIGINAL ARTICLE

CLINICAL ORAL IMPLANTS RESEARCH WILEY

Hard and soft tissue healing around implants with a modified implant neck configuration: An experimental in vivo preclinical investigation

David Palombo[1] | Maryam Rahmati[2] | Fabio Vignoletti[1] | Javier Sanz-Esporrin[1,3] | Håvard Jostein Haugen[2] | Mariano Sanz[1,3]

[1]Section of Periodontology, Faculty of Odontology, University Complutense of Madrid, Madrid, Spain

[2]Department of Biomaterials, Institute of Clinical Dentistry, Faculty of Dentistry, University of Oslo, Norway

[3]ETEP (Etiology and Therapy of Periodontal and Peri-implant Diseases) Research Group, Madrid, Spain

Correspondence
Javier Sanz Esporrin, Section of Periodontology, Faculty of Odontology, University Complutense of Madrid, Plaza Ramón y Cajal, s/n, 28040 Madrid, Spain.
Email: javisanzes@gmail.com

Funding information
This study was partially funded through a research contract between Sweden/Martina Dental Implants SpA (Padova, Italy) and the University Complutense of Madrid (UCM)

Abstract

Objectives: Evaluate the dimensions and morphology of peri-implant tissues around a modified dental implant designed with tissue level connection and a convergent transmucosal neck, when compared with a conventional bone level implant connected to a cylindrical machined titanium abutment.

Material and methods: Eight experimental animals were used for this in vivo investigation, in whom 16 test and 16 control implants were placed following a random allocation sequence. The following histological outcomes at 4 and 12 weeks were evaluated: morphology of peri-implant tissues, the soft tissue height and thickness, the horizontal and vertical bone remodeling, and the bone to implant contact (BIC).

Results: In both early (4 weeks) and late (12 weeks) healing times, there were no statistically significant differences between test and control implants, with respect to the overall height and thickness of the peri-implant hard and soft tissues. There was a tendency toward a more coronal free gingival margin (I-FGM) at the buccal aspect of test when compared to control implants (at 4 weeks, difference of 0.97 mm ($p = .572$) and 0.30 mm ($p = 1.000$) at 12 weeks). Similarly, there was a tendency toward a more coronal position of the first bone to implant contact (I-B) at the buccal aspect of test as compared to control implants (1.08 mm ($p = 0.174$) at 4 weeks and 0.83 mm ($p = 0.724$) at 12 weeks).

Conclusions: Hard and soft tissue healing occurred at both implant types with no statistically significant differences. Test implants tended to present a more coronal gingival margin (FGM) and first bone to implant contact (B).

KEYWORDS
animal experiments, bone implant interactions, morphometric analysis, soft tissue-implant interactions

Palombo and Rahmati Contributed equally to this study.

1 | INTRODUCTION

The transmucosal component of a dental implant is the area located between the first bone to implant contact and the soft tissue free mucosal margin (Berglundh & Lindhe, 1996). Depending on the implant design, this space can be occupied by either a polished neck that is part of the implant fixture (tissue level implants), an abutment connected to the implant platform located at the bone level (bone level implants), or a combination of implant neck and abutment, where the position of the implant to abutment junction resides within the transmucosal area (tissue level implants with subgingival connection).

Once an abutment is connected to the implant, the implant's design to abutment interface and its location within the transmucosal area may affect the morphogenesis of peri-implant mucosa and the marginal peri-implant bone remodeling processes during healing (Berglundh et al., 2007; Hermann et al., 2001). Thus, to maintain a stable mucosal height (Berglundh & Lindhe, 1996; Linkevicius et al., 2015), with adequate thickness (Cosyn et al., 2016; Jung et al., 2007), and a minimal loss of peri-implant bone (Hermann et al., 2001; Nevins et al., 2008; Strietzel et al., 2015), implant industry has introduced various innovations in the macro- and micro-geometry of the implant necks, abutments, and prosthetic connections, with the goal of providing favorable conditions for healing and long-term hard and soft tissue stability within this transmucosal area.

Recently, a new implant design was introduced by Sweden & Martina SpA, the Prama® Implant, characterized by a tissue level connection with a specific transmucosal convergent implant neck configuration and a modified surface. This design seeks to (a) locate the implant-abutment connection away from the bone crest (Hermann et al., 2001); (b) create more horizontal space for increasing the thickness of the peri-implant soft tissues (Cocchetto & Canullo, 2015; Hakkinen et al., 2000; Souza et al., 2018); and (c) provide a modified surface aimed to promote early fibroblast adhesion and the establishment of a stable connective tissue seal (Chehroudi et al., 1992; Doyle et al., 2009; Guillem-Marti et al., 2013; Nevins et al., 2008).

This innovative implant design has only been evaluated in non-controlled clinical studies, reporting favorable performance in terms of marginal soft tissue stability, stable marginal bone levels, and appropriate esthetic outcomes assessed through Pink Esthetic Score (PES), after 10, 18, and 36 months (Cabanes-Gumbau et al., 2019; Canullo et al., 2017; Cocchetto & Canullo, 2015). These clinical studies, however, cannot ascertain whether these outcomes are related to the innovative features of this implant and how its new design may influence the healing of the peri-implant tissues, in comparison with standard bone level implants connected to a conventional abutment.

It was therefore the objective of this in vivo preclinical investigation to compare the healing and integration of the peri-implant tissues around implants with an innovative neck configuration, compared to standard implants connected to abutments at the crestal bone level.

2 | MATERIAL AND METHODS

2.1 | Experimental design

This study was designed following the modified ARRIVE guidelines (Appendix S1) for reporting experimental preclinical investigations (Vignoletti & Abrahamsson, 2012) and in compliance with the current Spanish and European Union regulation (European Communities Council Directive 86/609/EEC) regulating in vivo experimentation. The experimental phase of this investigation was conducted at the "Centro de Cirugía de Mínima Invasión Jesús Usón" in Caceres, Spain, once the study protocol had been approved by the local Ethical Committee (REGA code: ES 100370001499). Test and control implants were inserted in both hemi-mandibles using a randomized block group distribution.

2.2 | Sample and facilities

Eight adult beagle dogs between 1.5 and 2 years old and with a weight ranging between 10 and 20 kg were housed in purpose-designed kennels in a 12:12 light/dark cycle and 22–21°C and were fed on a soft pellet diet. Every animal received an identification code printed in a sub-cutaneous RFID chip. Experienced veterinary doctors monitored the experimental animals during the entire course of this investigation.

2.3 | Test and control dental implants

Test and control implants had the same diameter (3.3 mm) and length (8.5 or 10 mm) and their endosseous component presented the same moderately rough Zirconium Sand-Blasted Acid Etched Titanium surface (ZirTi®, Sweden & Martina), with a mean Sa value of 1.3 μm. Figure 1 depicts the different transmucosal design in test and control implants.

The test implants presented a 2.8 mm neck with a cylindrical configuration in the first 0.8 mm and a convergent one in the most coronal 2 mm. Its diameter scaled from 3.4 mm at the bone level to 3.0 mm at the most coronal point, and its surface was covered by unilaterally oriented micro-grooves of 60 μm (Ultrathin Threaded Microsurface—UTM). These implants have been specifically manufactured for this study with a reduced diameter of 3.3 mm, to better suit the anatomy of the animals adopted, although they presented the same macro- and micro-structural characteristics of the commercially available Prama® implant (Sweden & Martina). The control implants (Premium One, Sweden & Martina) were commercially available bone level implants with a 0.8 mm cylindrical neck also provided with the UTM surface (Figure 1). Both test and control implants received platform matched, cylindrical, hollow abutments with a central screw, and an internal hexagonal connection (Collex One®, Sweden & Martina).

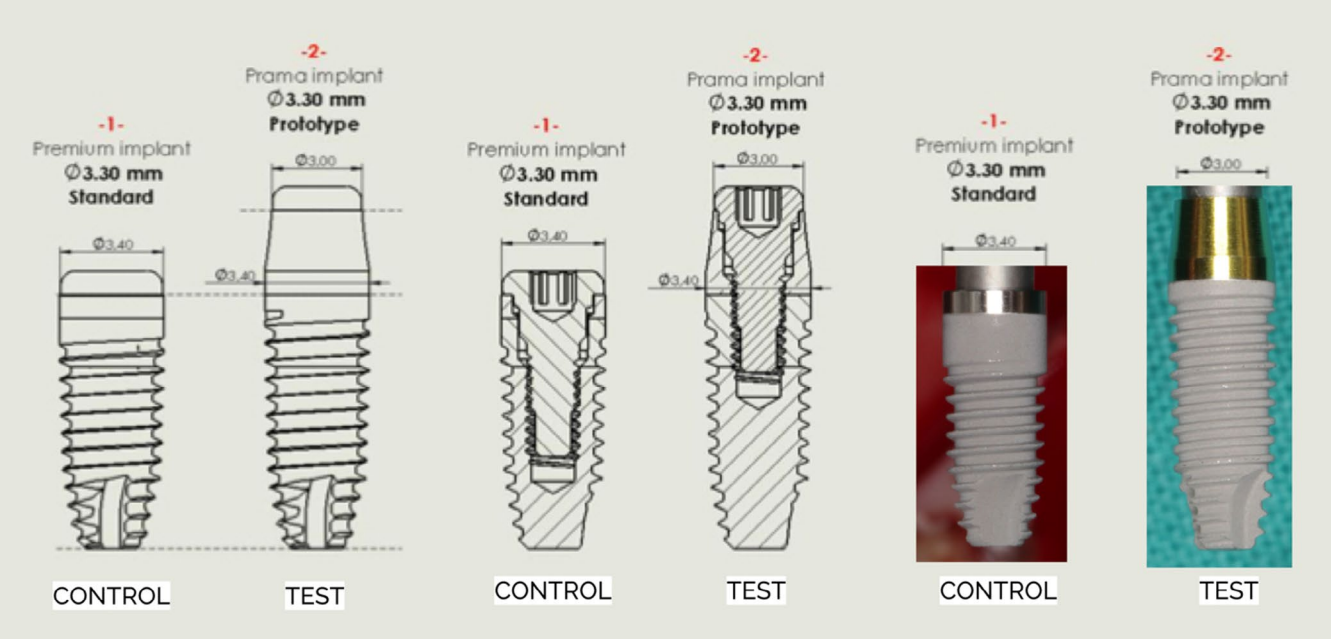

FIGURE 1 Schematic representation of the test and control implants adopted in the experimental phase

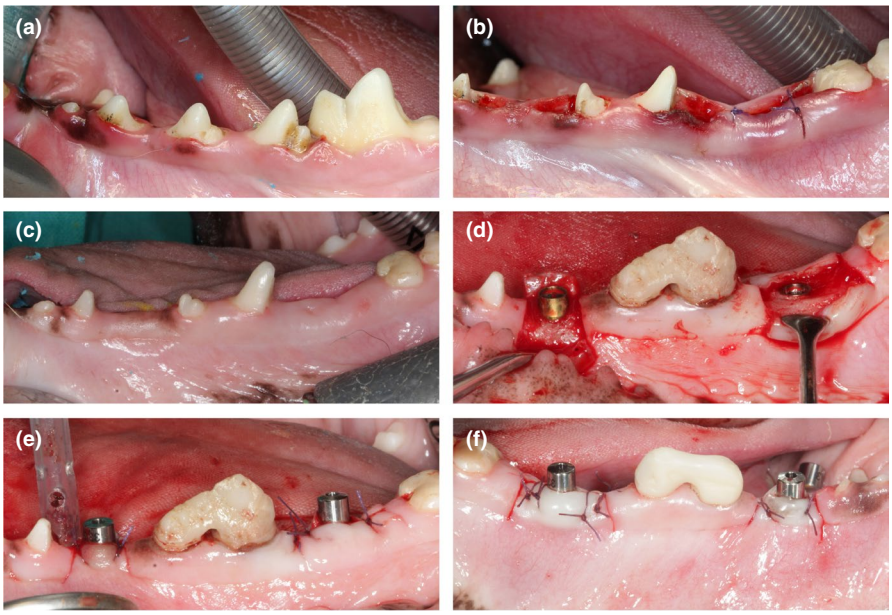

FIGURE 2 Surgical sequence of the experimental protocol. (a) baseline situation; (b) 1st surgery: extraction of the mesial root of 1M1 and 3P3, and the distal one of 4P4 and 2P2; (c) 8 weeks healing; (d) placement of test and control implants in the mesial alveolus of 1M1 and in the distal one of 2P2; (e) immediate postoperative view after implant placement; (f) implant placement in the contralateral side, 8 weeks afterwards

2.4 | Surgical procedures

2.4.1 | Intervention 1. Root extractions

Using a computer-generated random allocation sequence, in one hemi-mandible of each experimental animal 1M1, 4P4, 3P3, and 2P2 were hemisected and the mesial root of 1M1 and 3P3 and the distal of 4P4 and 2P2 were atraumatically extracted. After the endodontic treatment of the roots remaining in the alveolar bone, the adjacent sockets were left to heal spontaneously, thus resulting in two edentulous sites in each hemi-mandible (Figure 2a,b).

2.4.2 | Intervention 2. Root extractions and implant placement.

Eight weeks after the first intervention, the contralateral hemi-mandible received the same extraction and endodontic treatment protocol as in the first intervention. While in the other hemi-mandible one test and one control implant were placed according to the randomization sequence, in the healed crests of the mesial root of 1M1 and the distal of 2P2, using a non-submerged standard implant placement protocol. In brief, after mid-crestal incisions and elevation of full-thickness buccal and lingual flaps, implant site preparation was carried out according to the drilling

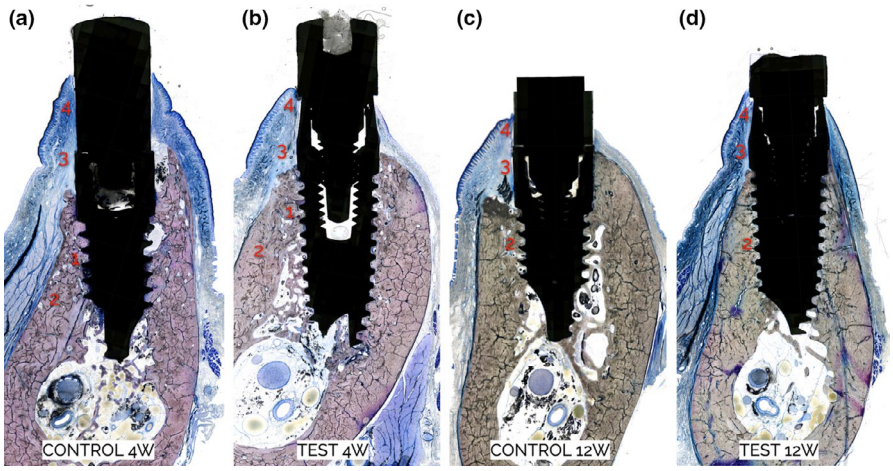

FIGURE 3 Buccolingual histologic ground sections representing: (a) Control implants at 4 weeks; (b) Test implants at 4 weeks; (c) Control implants at 12 weeks; (d) Test implants at 12 weeks, with the surrounding tis-sues. (1) Woven bone; (2) Lamellar bone; (3) Connective tissue contact; (4) Barrier Epithelium

sequence recommended by the manufacturer. During the implant insertion, the buccal bone crest was used to guide the final apico-coronal position of each implant. In test implants, the interphase between the rough and UTM surface of the implant was placed at the level of the buccal bone crest, while in control implants, the platform was placed juxtacrestally. Once the implants were inserted, they received a cylindrical transmucosal healing abutment and flaps were adapted and sutured around them using simple interrupted sutures (5/0, PGA; Figure 2c,d).

Within the same surgical session, the residual mesial root of 4P4 and the distal one of 3P3 were prepared with either a long chamfer technique or a biologically oriented preparation technique (BOPT), according to the randomization sequence, and received an immediate PMMA provisional.

2.4.3 | Intervention 3. Implant placement

Eight weeks after intervention 2, the same implant placement and tooth preparation protocols were replicated in the contralateral hemi-mandibles. (Figure 2f).

2.5 | Post-surgical care

After each surgical intervention, analgesic and antibiotic medications were administered. Animals were fed with a soft diet, and plaque control was assured by using a solution of chlorhexidine 0.12% and CPC 0.05% (PerioAid Tratamiento, Laboratorios Dentaid) sprayed on both hemi-mandibles two days per week. Furthermore, once a week, the surgical areas were brushed using a conventional manual toothbrush and a chlorhexidine solution. At these weekly visits, the status of the peri-implant tissues was assessed and if inflammation was present it was documented.

2.6 | Euthanasia

Animals were sacrificed four weeks after the last surgical intervention with an overdose of sodium pentothal (40–60 mg/kg/i.v., Dolethal, Vetoquinol). Each animal provided two hemi-mandibles with 4 and 12 weeks healing periods, respectively, which were freed from their attached tissues and cut into halves by sectioning between the central incisors. Each hemi-mandible was placed into a sealable sample container containing 4% formalin solution, which were stored in a secure area at constant temperature (5°C) from the time of collection until they were shipped for histological processing.

From each hemi-mandible, 4 tissue blocks were obtained: 2 containing test or control implants with the surrounding tissues, and 2 containing teeth prepared with a chamfer or BOTP technique with the surrounding tissues.

2.7 | Histological processing

The tissue blocks from one randomly selected animal were processed by decalcification following a modification of the "fracture technique" (Berglundh et al., 1994), while the remaining blocks were processed by ground sectioning following the methodology described by Donath & Breuner (1982). Specimens allocated to the ground section technique were dehydrated in a graded series of ethanol and embedded in methyl methacrylate (MMA). One section of each implant was cut in a buccolingual plane, and the central section was further grounded and polished to a final thickness of approximately 70 μm (Exakt). Obtained sections were then stained using the Levai Laczko staining method (Figure 3).

Only sections from dental implants were analyzed in this study, while section from prepared teeth will be analyzed in a future publication.

2.8 | Histological analysis

High-resolution images of the ground sections were acquired using an automated slide scanner system (Axio Scan Z1, Carl Zeiss Microscopy) and assessed by histomorphometry in duplicate by two independent and calibrated examiners (DP and MR) using a dedicated image analysis software (Zen lite Blue software, Carl Zeiss Microscopy). Intraclass correlation coefficients were generated to

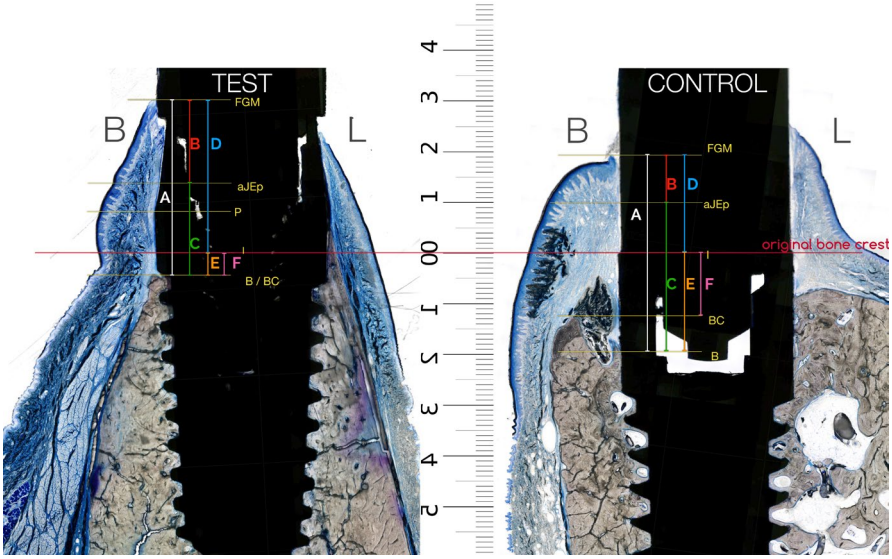

FIGURE 4 Histometric vertical measurements: A, Soft tissue height (PM-B); B, JEp height (PM-aJE); C, CT height (aJEP - B); D, Soft tissue margin (I-PM); E, First bone to implant contact (I - B); F, Bone Crest (I-Bc)

estimate the intra- and inter-examiner reproducibility. The mean from duplicate measurements was used for the analysis.

2.9 | Histological outcomes

2.9.1 | Histometric measurements of hard and soft tissues

The following landmarks were used in the histometric analysis:

- Shoulder of the implant. (I);

In test implants, the reference point was the interphase between the rough and UTM surface, located 2.8 mm apical to the implant shoulder.

- Marginal bone crest (Bc).
- Most coronal bone to implant contact (B).
- Margin of the peri-implant mucosa (PM).
- Apical border of the junctional epithelium (aJE).

The following vertical and horizontal distances were calculated on the buccal and lingual aspects of each implant and expressed in mm. (Figures 4 and 5).

a. Hard tissue measurements.

- Position of the first bone to implant contact (I-B).
- Position of the most coronal point of the alveolar bone crest (I-Bc).
- Width of the bone crest 1, 2, and 3 mm apically to the most coronal point of the crest (Bcw 1, 2, 3)

Horizontal distance from the implant and the outer surface of the bone crest 1, 2, and 3 mm apically to the most coronal point of the crest (Bc).

- Width of the bone crest 1mm apical to the implant platform (Bcwl 1).

Horizontal distance from the implant and the outer surface of the bone crest, 1mm apical to the implant platform (I);

a. Soft tissue measurements.

- Height of the supra-crestal soft tissues (PM-B)
- Height of the barrier epithelium (PM-aJE)
- Height of the connective tissue contact (aJE-B)
- Position of the free gingival margin (I-PM)
- Width of the peri-implant mucosa at the implant platform (PMwI)

Horizontal distance from the implant profile to the oral epithelium of the peri-implant mucosa, at the level of the implant platform (I).

- Width of the peri-implant mucosa 1, 2, and 3 mm apically to the PM (PMw1, 2, and 3)

Horizontal distance from the abutment implant profile, or bone crest and the oral epithelium of the peri-implant mucosa 1, 2, and 3 mm apically to the free gingival margin (PM).

2.10 | Bone to implant contact

The percentage of bone to implant contact (BIC) was calculated along the buccal and lingual aspect of test and control implants

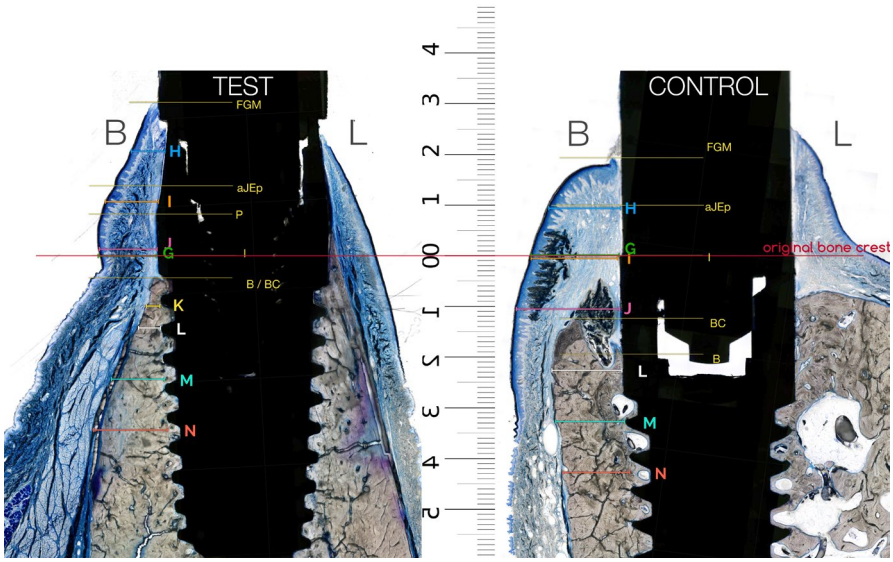

FIGURE 5 Histometric horizontal measurements: G, Soft tissue thickness at implant platform (PMwI); H, Soft tissue thickness 1 mm apical to FGM (PMw1); I, Soft tissue thickness 2 mm apical to FGM (PMw2); J, Soft tissue thickness 3 mm apical to FGM (PMw3); K, Bone thickness 1 mm apical to the implant platform (BcwI 1); L, Bone thickness 1 mm apical to BC (Bcw 1); M, Bone thickness 2 mm apical to BC (Bcw 2); N, Bone thickness 3 mm apical to BC (Bcw 3)

in both the most coronal third (3 mm) and the whole dimension of the implant. BIC at the level of the UTM surface was also measured.

2.11 | Statistical analysis

Outcome measurements were expressed in means and standard deviations (±SD), considering the experimental animal as the unit of analysis. After performing normality tests (Shapiro–Wilk test), if data followed a normal distribution, the one-way ANOVA test with Bonferroni correction was used to assess the differences between the test and control implants for all outcome measurements. If data were not normally distributed, the non-parametric test of Kruskal–Wallis was used. Differences were deemed statistically significant when p was <.05. The statistical analysis was performed using the software SPSS 24.0 (SPSS Inc.).

3 | RESULTS

3.1 | Clinical outcomes

In 7 of the 8 experimental animals, the healing was uneventful. Their behavior, as well as their eating and drinking habits remained normal throughout the course of experimental period. In this group, all implants achieved osseointegration and remained in place until the end of the experimental period. One experimental animal (#5) died during the study due to endometriosis.

3.2 | Descriptive histology

As reported in the methodology section, in one randomly selected experimental animal (#7), all specimens were decalcified to be processed by thin sectioning and immunohistochemistry. This manuscript reports the results from the implants placed in the remaining 6 experimental animals (#1, 2, 3, 4, 6, 8), where specimens were processed by ground sectioning and descriptive histology and histometric measurements were obtained. At 4 weeks, in both test and control implants, the bone to implant contact was present across the whole implant surface, with a variable amount of woven bone, mainly located at the inter-thread

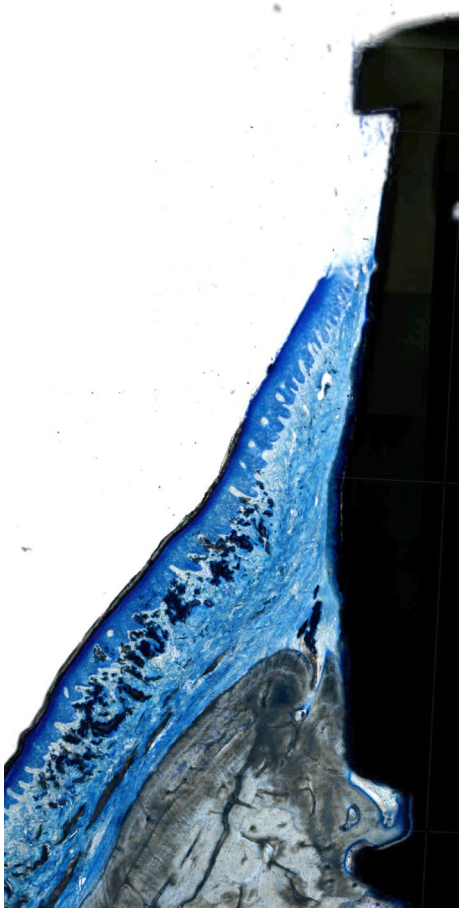

FIGURE 6 Lingual section of a test implant at 12 weeks of healing: general view

spaces. At 12 weeks, both test and control implants depicted mature lamellar bone distributed along the entire implant surface.

Supracrestally, both groups exhibited a healthy peri-implant mucosa characterized by a barrier epithelium of variable length and a connective tissue in tight apposition with the transmucosal implant components (neck, abutment, or exposed implant surface). There were no signs of frank inflammation, (Figure 3).

In the test implants, using a polarized filter, two groups of collagen fibers were distinguishable on the sagittal plane within the connective tissue in the vicinity with the implant surface: an external group with fibers running parallel to the transmucosal implant components and being inserted in the periosteum, and an internal group without a distinct orientation, but being sectioned perpendicularly, what suggests a circular orientation around the implant neck/abutment (Figures 6 and 7). Such finding was not observed around the polished abutments connected to control implants, where the collagen fibers were mostly oriented parallel to the implant abutment (Figures 8 and 9).

3.3 | Histometric measurements

Results from the histometric measurements are presented in Tables 1-3.

The intra-examiner intra-class correlation coefficient was 0.995 (95% confidence intervals: 0.974–0.999) for DP and the inter-examiner intra-class correlation coefficient between DP and MR was 0.859 (95% confidence intervals: 0.629–0.946).

3.3.1 | Bone to implant contact

Bone to implant contact results are presented in Table 1.

At 4 and 12 weeks of healing, a similar BIC percentage was observed at both test and control implants. Also, similar BIC percentages at the most coronal 3 mm of the implants were observed in both implant groups (Table 1). BIC was also observed along some sections of both test and control implants, at the level of the UTM surfaces (Figure 10).

3.3.2 | Position of the first bone to implant contact (I-B)

These histometric measurements are presented in Tables 2-3.

At 4 weeks, the position of the first bone to implant contact was approximately 1mm more coronal in the test compared to control implants, both at the buccal ($\Delta = 1.08$ mm, $p = .174$) and lingual ($\Delta = 1.09$ mm, $p = .137$) aspects, although these differences were not statistically significant. At 12 weeks, a similar difference was observed at the buccal aspect between test and control implants ($\Delta = 0.83$ mm; $p = .724$), although these differences were not statistically significant.

3.3.3 | Position of the alveolar bone crest in relation to the implant shoulder (I-BC)

At 4 weeks, the mean I-BC at test implants was of 0.20 (DS: 0.49) mm and 0.24 (DS: 1.11) mm at the buccal and lingual aspects, respectively. The corresponding values at control implants were 0.19 (DS: 0.49) and 1.34 (DS: 0.81) mm. A tendency toward statistical significance could be observed at the buccal aspect ($\Delta = 1.14$ mm; $p = .077$). After 12 weeks, a similar trend was observed, although not reaching statistical significance ($\Delta = 0.48$ mm buccally and 0.08 mm lingually; $p = 1.000$).

3.3.4 | Thickness of the bone crest (Bcw 1, 2, 3; Bcwl 1)

At each of the four reference points (Bcw 1, 2, 3; Bcwl 1), after 4 weeks, test implants presented a higher buccal bone thickness ($\Delta = 0.25$ mm ÷ 0.61 mm), but these differences did not reach statistical significance ($p > .05$).

At 12 weeks, the buccal bone crest at control implants was thicker than at test ones, 1, 2, and 3 mm apically from BC ($\Delta = 0.07$ ÷ 0.52 mm). However, when assessing the bone thickness 1mm apical to the implant platform (Bwl 1), test implants still exhibited a thicker bone crest ($\Delta = 0.17$ mm; $p = 1.000$). No statistically significant differences were detected in any of the comparisons.

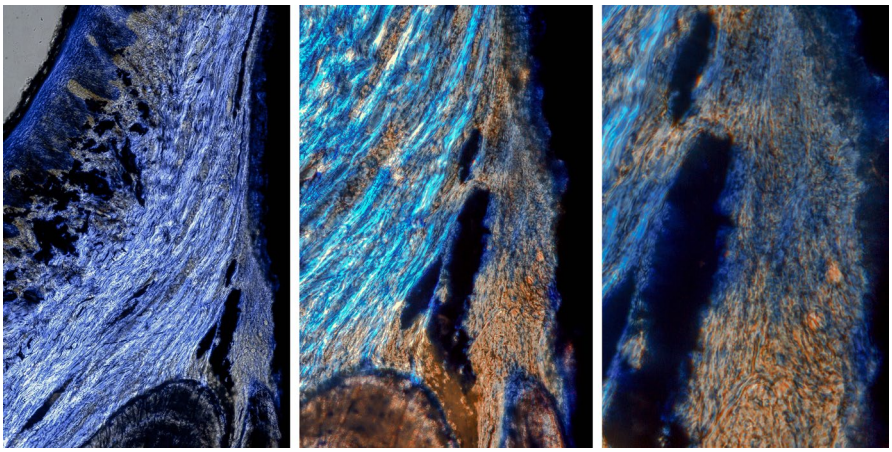

FIGURE 7 Lingual section of a test implant at 12 weeks of healing: 10x, 20x, and 40x images acquired with a polarized filter, revealing the spatial organization of the collagen tissue fibers with the connective tissue contact

3.3.5 | Height of the supra-crestal soft tissues (PM-B)

At 4 weeks, the mean soft tissue height at test implants was 3.06 (DS: 0.49) mm and 2.32 (DS: 0.48) mm at the buccal and lingual aspects, respectively. No statistically significant difference was observed when compared with control implants (Δ = −0.24 and −0.9 mm; p = 1.000 and .726). A similar pattern was observed at 12 weeks, again without significant differences between groups. (Tables 2 and 3).

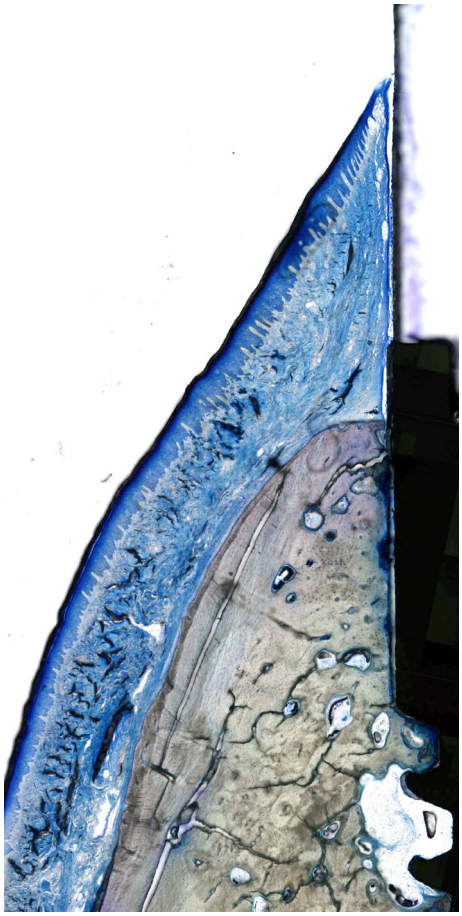

FIGURE 8 Lingual section of a control implant at 12 weeks of healing

3.3.6 | Height of the barrier epithelium (PM-aJE) and connective tissue adhesion (aJE-B)

No statistically significant nor clinically relevant differences could be observed at both healing times between test and control implants regarding the mean height of the barrier epithelium. A small non-significant difference in the connective tissue height was observed, with the control group having a longer CT dimension at the lingual aspect at 4 weeks (Δ = −0.99; p = .214) and at the buccal 12 weeks (Δ = −0.79; p = 1.000).

3.3.7 | Position of the free gingival margin (I-PM)

At 4 weeks, the free gingival margin at test implants was in a more coronal position compared to control implants, both at the buccal (Δ = 0.97 mm; p = .572) and lingual (Δ = 0.23 mm; p = 1.000) aspects, but these differences were not statistically significant.

At 12 weeks, a smaller difference was still present in favor of the test group, both at the buccal (Δ = 0.30 mm; p = 1.000) and lingual aspects (Δ =0.037 mm; p = 1.000), but again these differences were not statistically significant.

3.3.8 | Width of the peri-implant mucosa at the implant platform (PMw I; 1, 2, 3)

At each of the four reference points, an increased soft tissue thickness was observed at the buccal aspect of test implants at 4 weeks (Δ 0.42 mm to 0.53 mm), albeit non-statistically significant (p > .05). However, such pattern was inverted at 12 weeks, where the control group presented thicker buccal tissues at each of the four reference points (Δ 0.30 mm to 0.64 mm), again with no statistical significance. (Tables 2 and 3).

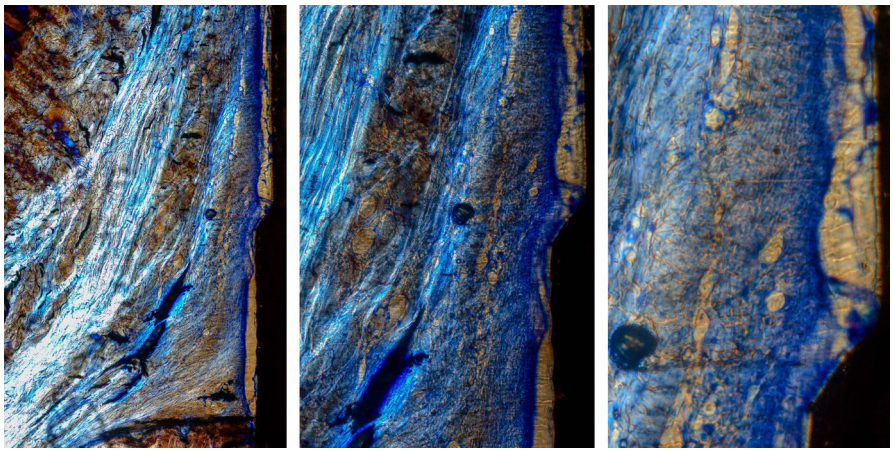

FIGURE 9 Lingual section of a control implant at 12 weeks of healing: 10x, 20x, and 40x images acquired with a polarized filter, revealing the spatial organization of the collagen tissue fibers with the connective tissue contact

TABLE 1 Bone to implant contacts at 4 and 12 weeks

	BIC buccal		BIC lingual		BIC merged		Coronal BIC buccal		Coronal BIC lingual		Coronal BIC merged	
	Mean (%)	SD (%)	Mean (%)	SD (%)	Mean (%)	SD (%)	Mean (%)	SD (%)	Mean (%)	SD (%)	Mean (%)	SD (%)
Prama 4W	68.263	26.069	56.301	18.620	62.282	21.342	58.778	33.651	55.309	17.897	57.042	25.162
Premium 4W	60.810	9.407	64.374	3.483	62.592	5.919	51.722	20.958	53.755	20.149	52.739	18.939
Prama 12W	76.059	20.539	76.247	13.496	76.153	14.788	64.209	26.702	75.223	21.820	69.716	20.124
Premium 12W	66.415	11.079	85.301	1.954	75.859	4.947	44.260	24.436	76.186	14.339	60.223	5.187
p	.625		.022		.277		.736		.183		.555	

Abbreviations: BIC, bone-to-implant contact; 4W and 12W, 4 and 12 weeks healing times.

Intergroup statistically significant difference ($p < .05$).

Percentages of de bone-to-implant contact are expressed throughout the entire implant surface and the coronal (the more coronal 3 mm of implant surface) of the buccal and lingual sides, and of the overall implant surface.

4 | DISCUSSION

The aim of the present experimental in vivo investigation was to study the hard and soft tissue integration around experimental implants with an innovative neck design, presenting a cylindrical/convergent profile, a microgrooved surface (UTM surface), and a tissue level connection, which sets the implant abutment interface away from the bone crest (Prama®, Sweden & Martina). This experimental implant was compared to a conventional bone level implant of identical diameter and length, provided with a microgrooved collar (also UTM surface), and connected to cylindrical, machined transmucosal abutments at juxta-crestal level (Premium One, Sweden & Martina).

The results reported in this manuscript showed that both at early and late healing stages, the biological processes leading to the implant osseointegration and to the morphogenesis of the peri-implant mucosae occurred similarly at the interface of both implants. This was in line with the clinical findings reported in the non-controlled studies available in the literature (Cabanes-Gumbau et al., 2019; Canullo et al., 2017; Cocchetto & Canullo, 2015). Nevertheless, it was a consistent finding that at test implants, both at 4 and 12 weeks of healing, the coronal margin of the peri-implant mucosa (PM) and the first bone to implant contact (B) were located more coronally as compared to control implants. Such finding was also associated with a thicker buccal bone and soft tissues at test implants at 4 weeks, difference that disappeared at late healing (12 weeks). Hence, while at 4 weeks, test implants exhibited thicker and more coronal buccal hard and soft tissues, at 12 weeks, the hard and soft tissues where still more coronal, but thinner when compared with control implants (Figures 11 and 12). The thicker buccal bone in control implants at 12 weeks may be related to a more pronounced vertical resorption of the buccal bone crest during healing, compensated with a thicker and apically displaced alveolar process.

The maintenance of a more coronal PM and B at test implants could be related to the shift of the implant to abutment connection from the bone level (control implants) to a more coronal position (tissue level implants). This is in line with data presented in the preclinical study by Hermann et al. (2001), where there was a more coronal position of B and PM (between 0.7 and 1 mm) in tissue level compared to bone level implants (Hermann et al., 2001).

Likewise, the new convergent neck geometry of test implants may also be responsible for a more coronal position of PM and B, as several lines of evidence support the idea that marginal bone remodeling may occur when there is insufficient horizontal or vertical space for the establishment of the peri-implant soft tissue complex. In agreement with this concept, Souza et al. (2018), compared implants with a 15° vs. 45° convex transmucosal profile resulting in lesser marginal bone loss (I-B = 0.89 ± 0.68 mm at wide abutments and 0.30 ± 0.30 mm at narrow ones; $p = .041$) in the implants with lesser abutment convexity (Souza et al., 2018). Similarly, experimental in vivo studies, clinical studies, and systematic reviews, have observed less marginal peri-implant bone loss around bone level implants receiving narrow, platform-switching abutments, as compared to conventional platform matched ones. (Cochran et al., 2009; Guerra et al., 2014; Strietzel et al., 2015). Even when comparing bone level implants with a narrow platform switched abutment (test) to conventional tissue level implants with a divergent transmucosal neck (control) in a RCT, platform-switching implants demonstrated significantly less radiographic marginal bone loss at 1 year (Fernandez-Formoso et al., 2012).

In the vertical dimension, the need of an adequate height for the establishment of the peri-implant mucosal seal has been demonstrated both in experimental and clinical studies, since in presence of thin peri-implant tissues (≤2 mm) a compensatory marginal bone resorption has been reported (Berglundh & Lindhe, 1996; Linkevicius et al., 2015). Hence, the lesser marginal bone remodeling observed around the convergent neck profile in test implants can be related to the combination of a tissue level design with the provision of more horizontal space for the establishment of the supra-crestal soft tissues.

Even though the reported differences between test and control implants did not reach statistical significance, they may be relevant clinically, what needs to be further investigated in adequately powered clinical studies, as preclinical investigations are usually

TABLE 2 Comparative statistics of the buccal and lingual measurements at 4 weeks

	Buccal						Lingual					
	Prama 4 weeks		Premium one 4 weeks		ANOVA		Prama 4 weeks		Premium one 4weeks		ANOVA	
Variable	Mean (mm)	SD (mm)	Mean (mm)	SD (mm)	I-J	*P*	Mean (mm)	SD (mm)	Mean (mm)	SD (mm)	I-J	*P*
PM-B	3.0631	0.485850	3.42210	0.883154	−0.359	1.000	2.32060	0.480182	3.22500	1.268530	−0.904	.716
PM-aJE	1.78920	0.705310	1.56340	0.478001	0.226	1.000	1.16100	0.408014	1.24700	1.009576	−0.086	1.000
aJE-B	1.68880	0.995968	2.02400	0.920234	−0.324	1.000	0.99084	0.788534	1.98480	0.830693	−0.994	.214
I-PM	3.05360	0.525791	2.08520	1.158124	0.968	.572	2.03560	0.948284	1.80140	1.104892	0.234	1.000
I-B	−0.39340	0.530774	−1.47780	0.769983	1.084	.174	−0.28840	1.086812	−1.37960	0.494633	1.091	.137
I-Bc	−0.19660	0.486044	−1.34080	0.812629	1.144	.077	−0.24040	1.112317	−0.42400	0.468162	0.184	1.000
PMwI	1.57120	0.546079	1.03960	0.480554	0.532	.375	0.99840	0.446943	1.03320	0.404798	−0.035	1.000
PMw1	1.10280	0.625516	0.68740	0.135559	0.415	.561	0.66040	0.178164	1.15600	0.937809	−0.496	.949
PMw2	1.56480	0.891085	1.10340	0.129548	0.461	.974	1.07120	0.182045	1.19020	0.114187	−0.119	1.000
PMw3	1.99520	0.704105	1.50860	0.248529	0.486	.799	1.04580	0.420352	1.12640	0.463826	−0.081	1.000
Bcw1	1.22693	0.538578	0.9736784	0.212066	0.253	1.000	1.28980	0.710702	1.36000	0.783292	−0.070	1.000
Bcw2	1.46460	0.367845	1.03660	0.262838	0.428	.596	1.75740	0.845969	1.83420	0.709659	−0.077	1.000
Bcw3	1.71220	0.382515	1.29100	0.206135	0.421	.678	2.06980	0.904542	2.11140	0.768871	−0.042	1.000
Bcwl 1	0.82720	0.688800	0.21720	0.303286	0.610	.267	1.33200	0.970864	1.22700	0.730659	0.105	1.000

Abbreviations: aJE-B, height of the connective tissue contact; Bcw1, width of the bone crest 1 mm apically to the most coronal point of the crest; Bcw2, width of the bone crest 2 mm apically to the most coronal point of the crest; Bcw3, width of the bone crest 3 mm apically to the most coronal point of the crest; Bcwl 1, width of the bone crest 1 mm apically to the implant platform; I-B, position of the first bone to implant contact; I-Bc, position of the most coronal point of the alveolar bone crest; I-PM, position of the free gingival margin; PM-aJE, height of the barrier epithelium; PM-B, height of the supra-crestal soft tissues; PMwI, width of the peri-implant mucosa at the implant platform; PMw1, width of the peri-implant mucosa 1 mm apically to the free gingival margin; PMw2, width of the peri-implant mucosa 2 mm apically to the free gingival margin; PMw3, width of the peri-implant mucosa 3 mm apically to the free gingival margin.

TABLE 3 Comparative statistics of the buccal and lingual measurements at 12 weeks

	Buccal						Lingual					
	Prama 12 weeks		Premium one 12 weeks		ANOVA		Prama 12 weeks		Premium one 12 weeks		ANOVA	
Variable	Mean (mm)	SD (mm)	Mean (mm)	SD (mm)	I-J	*P*	Mean (mm)	SD (mm)	Mean (mm)	SD (mm)	I-J	*P*
PM-B	3.29860	0.4338034	3.885078	0.153703	−0.525	1.000	1.87533	0.410554	2.18333	1.233455	0.308	1.000
PM-aJE	1.95483	0.956470	1.66000	0. 814179	0.295	1.000	0.93667	0.539240	0.89467	0.565191	0.042	1.000
aJE-B	1.36517	0.746826	2.15067	0.643771	−0.786	1.000	0.95217	0.359935	1.30500	0.729413	−0.353	1.000
I-PM	2.60250	0.678840	2.29833	1.078327	0.304	1.000	1.68550	0.609590	1.72200	945104	−0.037	1.000
I-B	−0.71000	0.470693	−1.53667	1.217276	0.827	.724	−0.22533	0.446512	−0.48000	0.355979	0.255	1.000
I-Bc	−0.63267	0.438635	−1.11333	0.897019	0.481	1.000	−0.10217	0.384677	−0.18633	0.545812	0.084	1.000
PMwI	1.09250	0.226446	1.39667	0.350009	−0.304	1.000	1.10017	0.512363	1.03300	0.419161	0.067	1.000
PMw1	0.76367	0.139909	1.09300	0.374621	−0.329	1.000	0.74950	0.289401	0.80733	0.237127	−0.058	1.000
PMw2	1.04100	0.181876	1.53400	0.380279	−0.493	1.000	1.00017	0.219998	0.83233	0.292386	0.168	1.000
PMw3	1.26133	0.365482	1.90567	0.557835	−0.644	.477	0.84350	0.101512	1.21767	1.020784	−0.374	1.000
Bcw1	0.557696	0.146700	1.06200	0.3315113	−0.518	.485	1.39700	0.750940	1.81033	0.900614	−0.413	1.000
Bcw2	0.78650	0.393211	1.075356	0.563037	−0.365	1.000	1.96117	0.965618	2.38867	1.016174	0.428	1.000
Bcw3	1.02750	0.357927	1.09400	0.689614	−0.067	1.000	2.36133	1.052500	2.80067	0.968368	−0.439	1.000
Bcwl 1	0.24567	0.346004	0.07967	0.137987	0.166	1.000	1.06767	0.391935	1.38333	0.204962	−0.159	1.000

Abbreviations: aJE-B, height of the connective tissue contact; Bcw1, width of the bone crest 1 mm apically to the most coronal point of the crest; Bcw2, width of the bone crest 2 mm apically to the most coronal point of the crest; Bcw3, width of the bone crest 3 mm apically to the most coronal point of the crest; Bcwl 1, width of the bone crest 1mm apically to the implant platform; I-B, position of the first bone to implant contact; I-Bc, position of the most coronal point of the alveolar bone crest; I-PM, position of the free gingival margin; PM-aJE, height of the barrier epithelium; PM-B, height of the supra-crestal soft tissues; PMw1, width of the peri-implant mucosa 1 mm apically to the free gingival margin; PMw2, width of the peri-implant mucosa 2 mm apically to the free gingival margin; PMw3, width of the peri-implant mucosa 3 mm apically to the free gingival margin; PMwI, width of the peri-implant mucosa at the implant platform.

underpowered in order to fulfill the animal welfare 3R concept (Replacement, Reduction, and Refinement).

When studying the bone to implant contact, both test and control implants demonstrated a high percentage of osseointegration.

Focusing on the UTM surface, when located subcrestally in the control implants, it allowed osseointegration (Figure 10), while when placed supracrestally in the test implants, this surface seemed to influence the special disposition of the connective tissue collagen fibers adjacent to the implant neck. Indeed, a fiber organization was observed in the test when compared with the control implants (Figures 7-10). These findings corroborate previous observations from in vitro investigations demonstrating the alignment of fibroblasts along the grooves of micro threaded surfaces, through a process denominated contact guidance (Lee et al., 2009; Walboomers et al., 2000). More specifically, it has been shown that surfaces with micro-grooves ≥50 μm, such as the UTM surface (60 μm), promote fibroblasts activation without inducing a fibrotic response (Guillem-Marti et al., 2013). However, these differences in the distribution of connective tissue fibers may also be consequence of the differences in the macro geometry between the transmucosal components of the test and control implants, and this fact needs further investigation.

In spite of these findings, none of the sections from the tested implants provided evidence of a peri-implant connective tissue attachment with inserted collagen fibers running perpendicular to the implant neck. These findings are in contrast with those reported by Nevins et al. (2008) describing supra-crestal connective tissue attachment at bone level implants with a neck containing Laser-Lok microchannels.

This preclinical in vivo investigation presents several limitations related to the use of an experimental animal model with a reduced sample size. Due to this fact, this study was unable to reject the null hypothesis as no statistical differences were found between treatment groups. This does not necessarily mean that the two neck designs perform equally, and hence, the conclusions should be interpreted mainly by their descriptive value.

Furthermore, the external validity of this study is limited by: (a) the absence of a provisional crown or an abutment with an anatomical emergence profile, which may further condition the peri-implant soft tissues; (b) the absence of any prosthetic load over the test and control implants; and (c) the absence of a platform-switching abutment at control implants.

Still, as the purpose of this study was to establish the influence of the test implant design on the establishment of the peri-implant mucosa and the related bone remodeling process, no load was applied to the implants, as such process commonly occurs in clinical practice without any loading. Furthermore, since one of the main characteristics of the test implant design is to provide more horizontal space to the supra-crestal tissues, through a convergent neck profile, a platform matched design was selected for the control group, in order to allow the experimental model to show the effect of such design characteristic in the establishment of the peri-implant mucosa.

Likewise, the internal validity of this comparative analysis is partially hampered by the presence of a different thread configuration at test and control implants in the most coronal part of the fixtures, as the threads in the test implants were extended more coronally as compared to the control one. Such difference was related by the implant manufacturer to the lack of adequate space for the implant chamber in the control implant, if adopting the same thread configuration of the test one, and may in part be responsible for the differences observed at the marginal bone level. Still, our research group demonstrated in a preclinical investigation using a similar experimental model that implants with different macro designs of their endosseous portion did not exhibit significant differences in marginal bone levels (de Sanctis et al., 2009).

Finally, the adopted study design allowed to assess the overall performance of the test implant over the control one, but not to explore the individual impact of each one of its main design characteristics (tissue level connection, convergent neck profile, UTM surface) on the healing of the peri-implant tissues, as for such purpose, at least three independent investigations should have been performed.

In conclusion, results from this study suggest that tissue level implants with a convergent transmucosal neck design presenting a

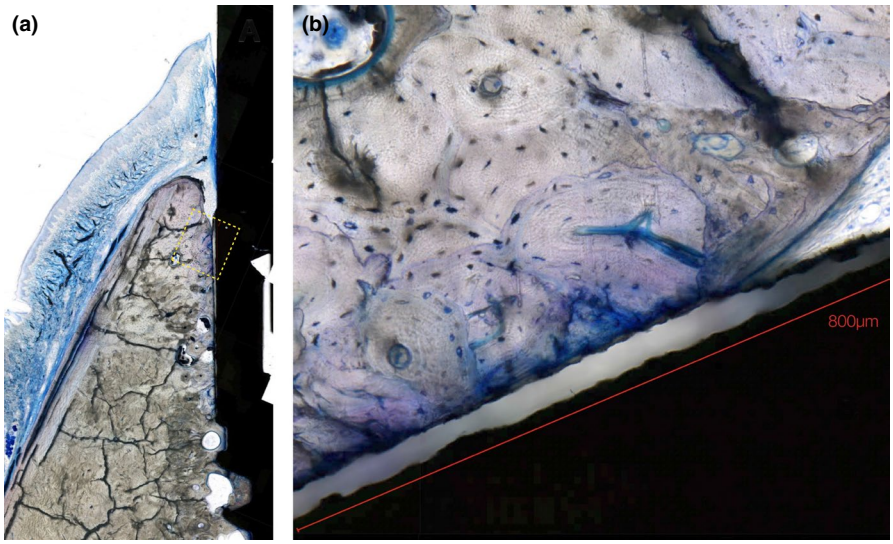

FIGURE 10 Lingual section of a control implant at 12 weeks of healing, revealing direct bone-to-implant contact over part of implant neck presenting a UTM surface: (a) general view; (b) UTM neck

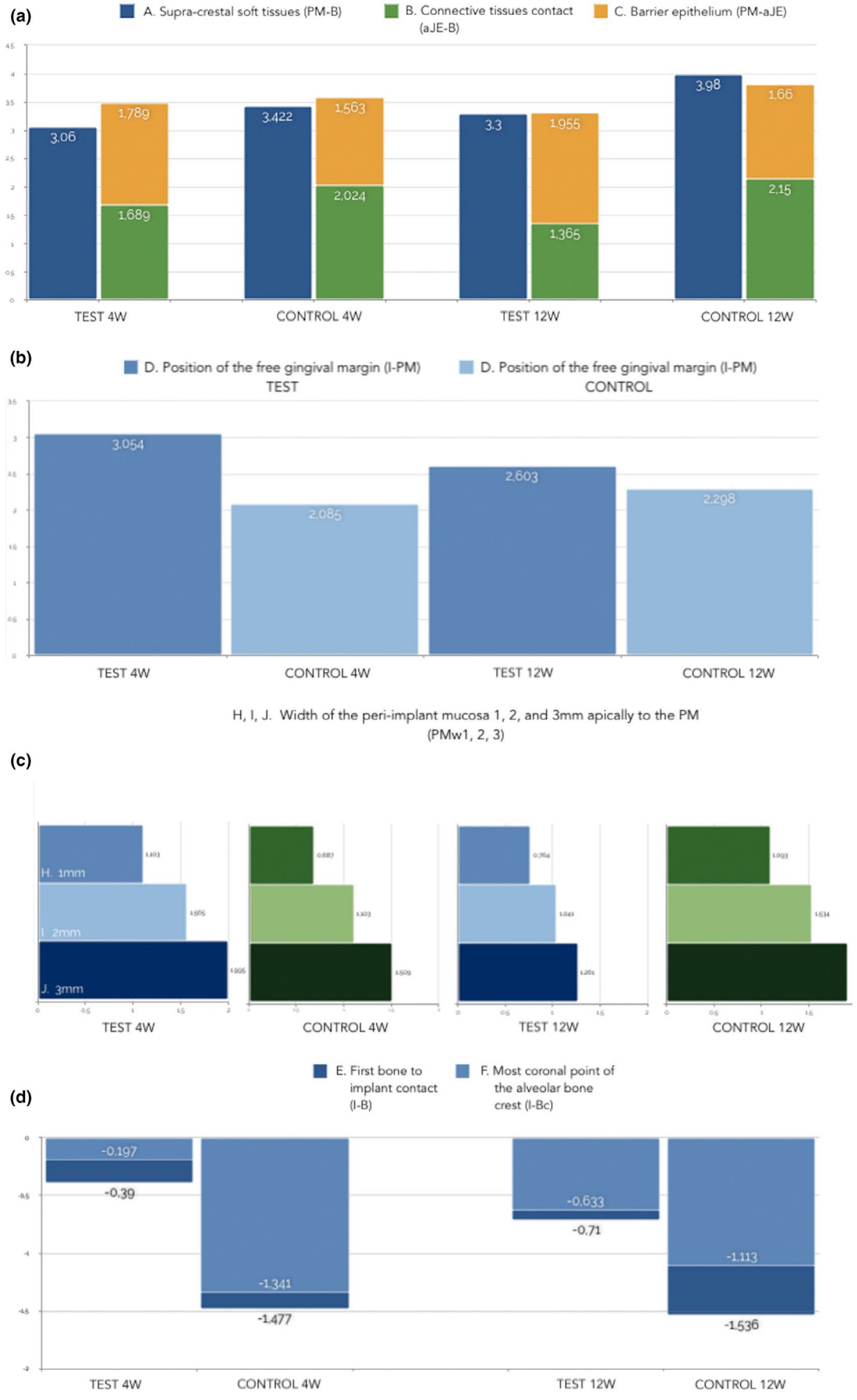

FIGURE 11 (a) Buccal soft tissue height, CT height and Ep height at test and control implants; (b) position of the buccal soft tissue margin relative to the implant platform at test and control implants (c) buccal soft tissue thickness 1, 2, and 3 mm apical to the free gingival margin; (d) position of B and BC relative to the implant platform at test and control implants

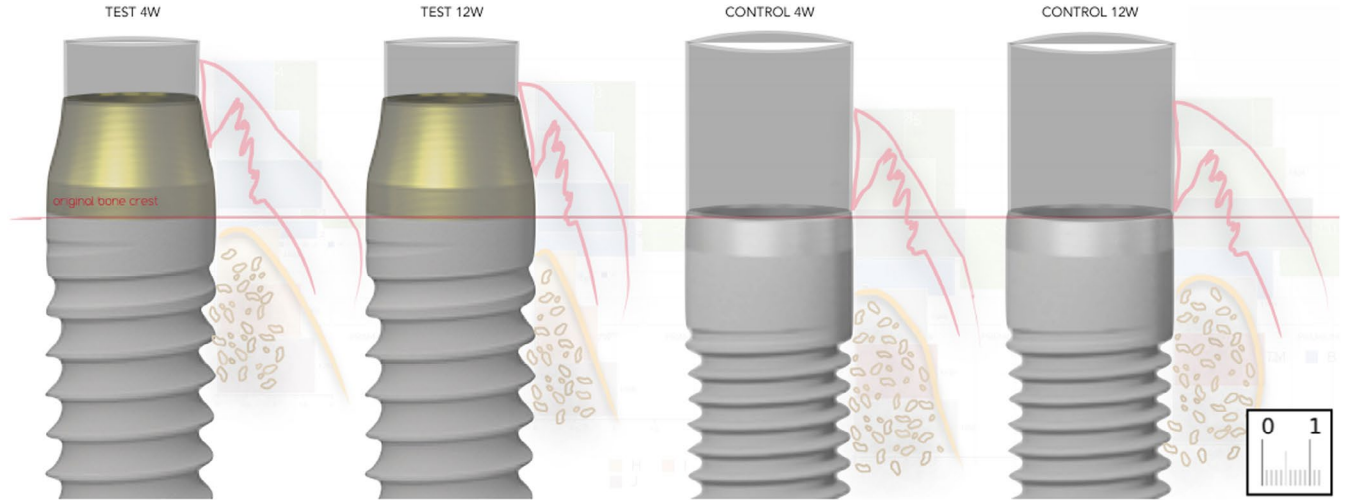

FIGURE 12 Scaled graphical representation of the buccal hard and soft tissues dimensions and position around test and control implants at 4 and 12 weeks of healing

UTM surface undergo equivalent processes of osseointegration and morphogenesis of the peri-implant mucosa, when compared to conventional bone level implants.

ACKNOWLEDGMENTS

Maryam Rahmati was supported by a project "Promoting patient safety by a novel combination of imaging technologies for biodegradable magnesium implants, MgSafe" funded by European Training Network within the framework of Horizon 2020 Marie Skłodowska-Curie Action (MSCA) grant number No 811226 (www.mgsafe.eu). Histological images were acquired at the Norbrain Slide scanning Facility at the Institute of Basic Medical Sciences, University of Oslo, a resource funded by the Research Council of Norway. Authors would like to acknowledge unvaluable contribution to the execution of the surgeries to Javier Núñez, Riccardo Di Raimondo, Sergio Martinez Villa, Fernando Luengo, and Rafa Pla. Also, authors would like to express their appreciation to personnel of the Jesús Usón Minimally Invasive Surgical Center research facilities, for their invaluable support with the care of the animals, specially to Francisco Javier Velas.

CONFLICT OF INTERESTS

All authors declare no conflict of interest.

AUTHOR CONTRIBUTIONS

David Palombo: Data curation (lead); Formal analysis (equal); Investigation (equal); Methodology (equal); Resources (equal); Writing-original draft (lead). **Maryam Rahmati:** Data curation (lead); Formal analysis (equal); Investigation (equal); Methodology (equal); Writing-review & editing (equal). **Fabio Vignoletti:** Conceptualization (lead); Data curation (equal); Investigation (equal); Methodology (equal); Resources (equal); Supervision (equal); Validation (equal); Visualization (equal); Writing-review & editing (equal). **Javier Sanz-Esporrin:** Data curation (lead); Formal analysis (lead); Investigation (equal); Methodology (equal); Resources (equal); Writing-review & editing (equal). **Håvard Jostein Jostein Haugen:** Data curation (equal); Investigation (equal); Methodology (equal); Resources (equal); Supervision (equal); Writing-review & editing (equal). **Mariano Sanz:** Conceptualization (lead); Funding acquisition (lead); Investigation (equal); Methodology (equal); Project administration (lead); Resources (equal); Supervision (lead); Validation (equal); Visualization (equal); Writing-review & editing (lead).

DATA AVAILABILITY STATEMENT

The data that support the findings of this study are available from the corresponding author upon reasonable request.

ORCID

Fabio Vignoletti https://orcid.org/0000-0002-4574-3671
Javier Sanz-Esporrin https://orcid.org/0000-0003-0859-3149
Håvard Jostein Haugen https://orcid.org/0000-0002-6690-7233
Mariano Sanz https://orcid.org/0000-0002-6293-5755

REFERENCES

Berglundh, T., Abrahamsson, I., Welander, M., Lang, N. P., & Lindhe, J. (2007). Morphogenesis of the peri-implant mucosa: an experimental study in dogs. *Clinical Oral Implants Research*, *18*(1), 1–8. https://doi.org/10.1111/j.1600-0501.2006.01380.x

Berglundh, T., & Lindhe, J. (1996). Dimension of the periimplant mucosa. Biological width revisited. *Journal of Clinical Periodontology*, *23*(10), 971–973. https://doi.org/10.1111/j.1600-051x.1996.tb00520.x

Berglundh, T., Lindhe, J., Jonsson, K., & Ericsson, I. (1994). The topography of the vascular systems in the periodontal and peri-implant tissues in the dog. *Journal of Clinical Periodontology*, *21*(3), 189–193. https://doi.org/10.1111/j.1600-051x.1994.tb00302.x

Cabanes-Gumbau, G., Pascual-Moscardo, A., Penarrocha-Oltra, D., Garcia-Mira, B., Aizcorbe-Vicente, J., & Penarrocha-Diago, M. A. (2019). Volumetric variation of peri-implant soft tissues in convergent collar implants and crowns using the biologically oriented preparation technique (BOPT). *Medicina Oral Patología Oral Y Cirugia Bucal*, *24*(5), e643–e651. https://doi.org/10.4317/medoral.22946

Canullo, L., Tallarico, M., Pradies, G., Marinotti, F., Loi, I., & Cocchetto, R. (2017). Soft and hard tissue response to an implant with a

convergent collar in the esthetic area: preliminary report at 18 months. *The International Journal of Esthetic Dentistry*, *12*(3), 306–323.

Chehroudi, B., Gould, T. R., & Brunette, D. M. (1992). The role of connective tissue in inhibiting epithelial downgrowth on titanium-coated percutaneous implants. *Journal of Biomedical Materials Research*, *26*(4), 493–515. https://doi.org/10.1002/jbm.820260407

Cocchetto, R., & Canullo, L. (2015). The "hybrid abutment": a new design for implant cemented restorations in the esthetic zones. *The International Journal of Esthetic Dentistry*, *10*(2), 186–208.

Cochran, D. L., Bosshardt, D. D., Grize, L., Higginbottom, F. L., Jones, A. A., Jung, R. E., Wieland, M., & Dard, M. (2009). Bone response to loaded implants with non-matching implant-abutment diameters in the canine mandible. *Journal of Periodontology*, *80*(4), 609–617. https://doi.org/10.1902/jop.2009.080323

Cosyn, J., Eghbali, A., Hermans, A., Vervaeke, S., De Bruyn, H., & Cleymaet, R. (2016). A 5-year prospective study on single immediate implants in the aesthetic zone. *Journal of Clinical Periodontology*, *43*(8), 702–709. https://doi.org/10.1111/jcpe.12571

de Sanctis, M., Vignoletti, F., Discepoli, N., Zucchelli, G., & Sanz, M. (2009). Immediate implants at fresh extraction sockets: bone healing in four different implant systems. *Journal of Clinical Periodontology*, *36*(8), 705–711. https://doi.org/10.1111/j.1600-051X.2009.01427.x

Donath, K., & Breuner, G. (1982). A method for the study of undecalcified bones and teeth with attached soft tissues. The Sage-Schliff (sawing and grinding) technique. *Journal of Oral Pathology*, *11*(4), 318–326. https://doi.org/10.1111/j.1600-0714.1982.tb00172.x

Doyle, A. D., Wang, F. W., Matsumoto, K., & Yamada, K. M. (2009). One-dimensional topography underlies three-dimensional fibrillar cell migration. *Journal of Cell Biology*, *184*(4), 481–490. https://doi.org/10.1083/jcb.200810041

Fernandez-Formoso, N., Rilo, B., Mora, M. J., Martinez-Silva, I., & Diaz-Afonso, A. M. (2012). Radiographic evaluation of marginal bone maintenance around tissue level implant and bone level implant: A randomised controlled trial. A 1-year follow-up. *Journal of Oral Rehabilitation*, *39*(11), 830–837. https://doi.org/10.1111/j.1365-2842.2012.02343.x

Guerra, F., Wagner, W., Wiltfang, J., Rocha, S., Moergel, M., Behrens, E., & Nicolau, P. (2014). Platform switch versus platform match in the posterior mandible - 1-year results of a multicentre randomized clinical trial. *Journal of Clinical Periodontology*, *41*(5), 521–529. https://doi.org/10.1111/jcpe.12244

Guillem-Marti, J., Delgado, L., Godoy-Gallardo, M., Pegueroles, M., Herrero, M., & Gil, F. J. (2013). Fibroblast adhesion and activation onto micro-machined titanium surfaces. *Clinical Oral Implants Research*, *24*(7), 770–780. https://doi.org/10.1111/j.1600-0501.2012.02451.x

Hakkinen, L., Uitto, V. J., & Larjava, H. (2000). Cell biology of gingival wound healing. *Periodontology 2000*, *24*(1), 127–152. https://doi.org/10.1034/j.1600-0757.2000.2240107.x

Hermann, J. S., Schoolfield, J. D., Nummikoski, P. V., Buser, D., Schenk, R. K., & Cochran, D. L. (2001). Crestal bone changes around titanium implants: a methodologic study comparing linear radiographic with histometric measurements. *International Journal of Oral and Maxillofacial Implants*, *16*(4), 475–485.

Jung, R. E., Sailer, I., Hammerle, C. H., Attin, T., & Schmidlin, P. (2007). In vitro color changes of soft tissues caused by restorative materials. *International Journal of Periodontics and Restorative Dentistry*, *27*(3), 251–257.

Lee, S. W., Kim, S. Y., Rhyu, I. C., Chung, W. Y., Leesungbok, R., & Lee, K. W. (2009). Influence of microgroove dimension on cell behaviour of human gingival fibroblasts cultured on titanium substrata. *Clinical Oral Implants Research*, *20*(1), 56–66. https://doi.org/10.1111/j.1600-0501.2008.01597.x

Linkevicius, T., Puisys, A., Steigmann, M., Vindasiute, E., & Linkeviciene, L. (2015). Influence of vertical soft tissue thickness on crestal bone changes around implants with platform switching: A comparative clinical study. *Clinical Implant Dentistry and Related Research*, *17*(6), 1228–1236. https://doi.org/10.1111/cid.12222

Nevins, M., Nevins, M. L., Camelo, M., Boyesen, J. L., & Kim, D. M. (2008). Human histologic evidence of a connective tissue attachment to a dental implant. *International Journal of Periodontics and Restorative Dentistry*, *28*(2), 111–121.

Souza, A. B., Alshihri, A., Kammerer, P. W., Araujo, M. G., & Gallucci, G. O. (2018). Histological and micro-CT analysis of peri-implant soft and hard tissue healing on implants with different healing abutments configurations. *Clinical Oral Implants Research*, *29*(10), 1007–1015. https://doi.org/10.1111/clr.13367

Strietzel, F. P., Neumann, K., & Hertel, M. (2015). Impact of platform switching on marginal peri-implant bone level changes. A systematic review and meta-analysis. *Clinical Oral Implants Research*, *26*(3), 342–358. https://doi.org/10.1111/clr.12339

Vignoletti, F., & Abrahamsson, I. (2012). Quality of reporting of experimental research in implant dentistry. Critical aspects in design, outcome assessment and model validation. *Journal of Clinical Periodontology*, *39*(Suppl 12), 6–27. https://doi.org/10.1111/j.1600-051X.2011.01830.x

Walboomers, X. F., Ginsel, L. A., & Jansen, J. A. (2000). Early spreading events of fibroblasts on microgrooved substrates. *Journal of Biomedical Materials Research*, *51*(3), 529–534. https://doi.org/10.1002/1097-4636(20000905)51:3<529:aid-jbm30>3.0.co;2-r

SUPPORTING INFORMATION

Additional supporting information may be found online in the Supporting Information section.

How to cite this article: Palombo, D., Rahmati, M., Vignoletti, F., Sanz-Esporrin, J., Haugen, H. J., & Sanz, M. (2021). Hard and soft tissue healing around implants with a modified implant neck configuration: An experimental in vivo preclinical investigation. *Clinical Oral Implants Research*, 32, 1127–1141. https://doi.org/10.1111/clr.13812